## Introduction

This application note describes a Digital Inrush Controller that combines IXYS digital power control technology and Zilog's 8-bit Z8F3281 MCU capabilities to illustrate a unique approach to control inrush current in AC-DC rectifiers or AC-DC converters. There are two objectives: first, to illustrate advantages of digital control that overcomes many of the disadvantages of the used right now technology, and second, to raise interests in digital control of the high power converters, potentially stimulating development of its next generation. IXYS digital control would allow the integration of control circuits and power devices on the same integrated circuit or semiconductor chip, according to the so-called "smart power" concept, which has a significant role in switched-mode power supply (SMPS) for achieving higher power densities.

Digital control allows distinctive solutions to control inrush current in typical AC-DC rectifier with capacitive load by limiting capacitor pre-charge current to a predetermined value at each half sine-wave cycle. Capacitor charge is spread over a number of cycles until capacitor is charged proportion of peak value of AC voltage source. Capacitor is charged according to time-dependent pulse train. The pulses are designed in a way to provide substantially equal voltage increment applied to capacitor to keep peak of charging current about the same value at each cycle. Number of cycles depends on capacitor value and charge current. For a given capacitor value which is selected depending on desired ripples amplitude, the charge current is a function of number of pulses and its timing position with respect to rectified sine wave. Detailed algorithm of creating pulse train for Digital Inrush Control is described in the Principles of Operation section.

IXYS Digital Inrush Controller features programmable overload protection and "Power Good" status signal. It is not sensitive to power outage, brownout and ambient temperature variations. It can operate with input voltage range from 80V to 240V AC and load current up to 3A. Entire operation process and essential values are fully programmable. The controller may be programmed to 50 Hz, 60 Hz or any other line input frequency operation.

This Digital Inrush Controller is valuable for high power loads with tens of Amperes of current in normal mode operation. It allows users to optimize the performance, maximize the efficiency across the load range and reduce the design time to market. IXYS power components allow handle pre-charge of load capacitors at this values while limit inrush current to controlled values.

## Main Features

This Digital Inrush Controller offers the following features:

- Input voltage range from 80V to 240V RMS
- Steady Load current up to 3A
- Programmable Overload protection
- Power Good status signal
- High endurance

- Not sensitive to power outage or brownout
- Not sensitive to ambient temperature variations
- Voltage ripples 15% at 2.5A load and output capacitance of 720µF
- Option to expand bulk capacitor value using external capacitors

## Potential Applications

It provides a basis for developing a variety of power management applications with IXYS power devices and MCU, including the following applications:

- AC/DC Power Supplies for computing server, storage network, industrial and medical.
- High Power AC-DC Rectifier
- High Power AC-DC PFC Converter

## Principles of Operation

This section describes a basic example of operation of a digital inrush controller. The device comprises typical power components of AC-DC rectifier (Diode Bridge, Inductor, and bulk Capacitor), switch Sw1 to commutate capacitor pre-charging current, switch Sw2 to connect/disconnect load, and digital control module based on Zilog's Z8F3281 MCU as shown on Figure 1. (Refer to Appendix A for actual circuit schematic and Appendix B for BOMs.)

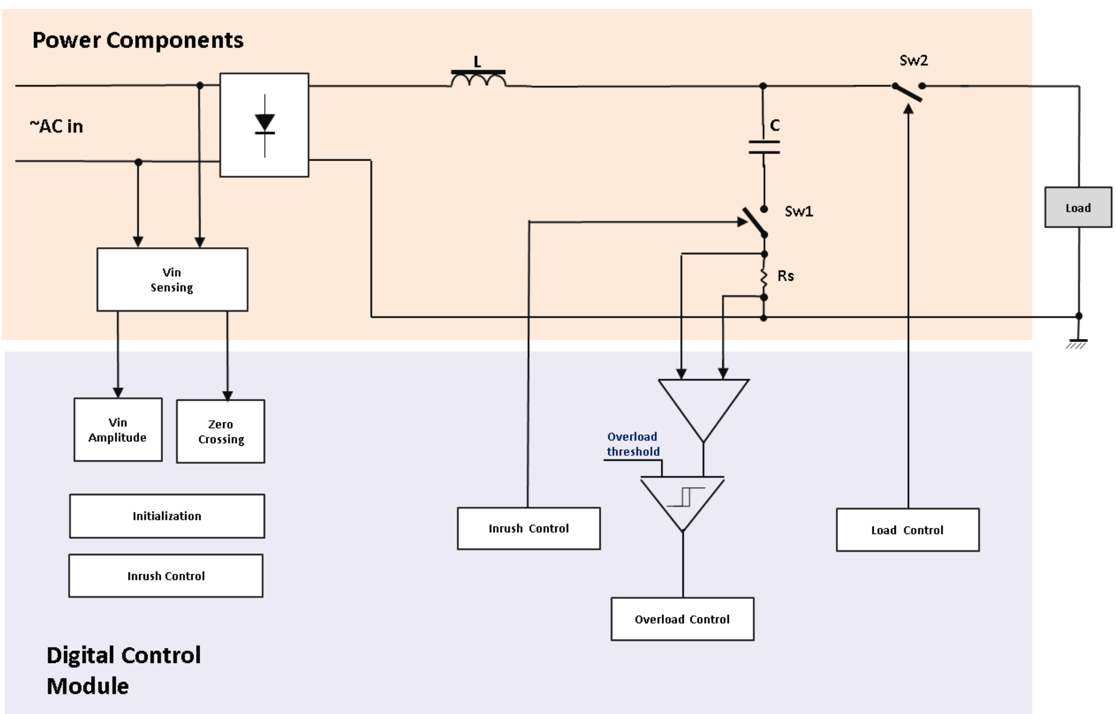


Figure 1: Functional Block Diagram of the Digital Inrush Controller

## Concept of Digital Inrush Control

Key point in the concept is to provide charge to bulk capacitor in equal increments. This is accomplished by providing control pulses to Sw1 (see Figure 1) in the way resulting in equal increments of a voltage applied to the bulk capacitor. It is possible to be done on a cycle by cycle basis considering cycle is half of sine wave of line voltage. Let us assign N cycles for inrush control operation, and then split normalized amplitude of sine wave cycle to N segments with increment of 1/N as shown on Figure 2.

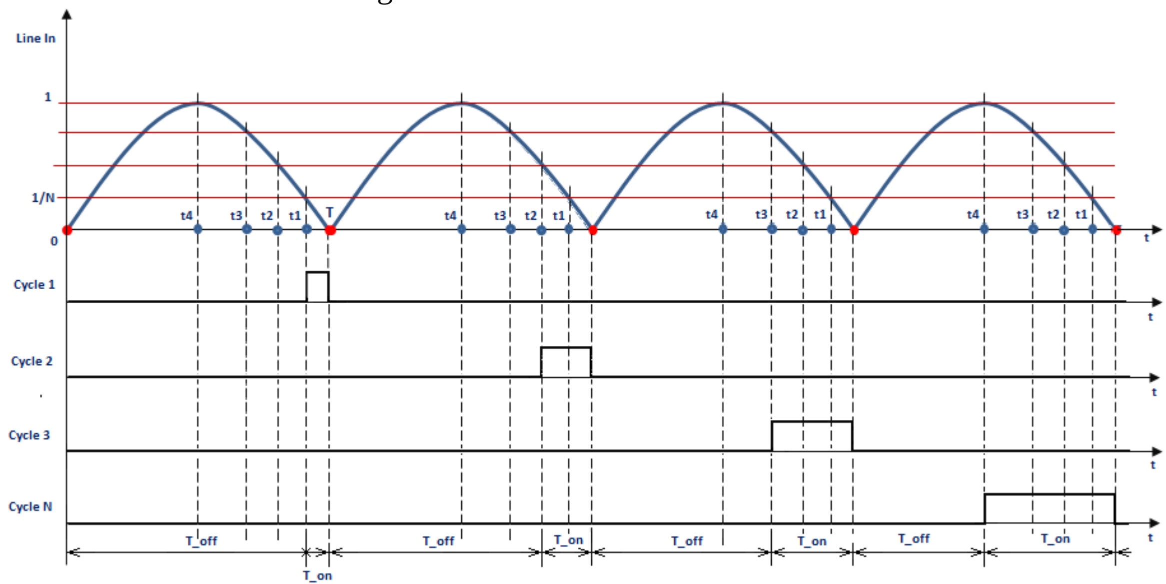


Figure 2: Digital Inrush Control timing

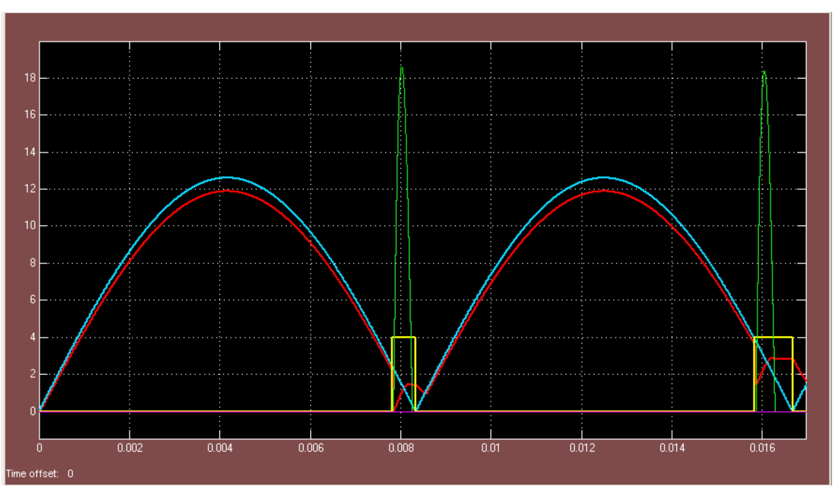


Figure 3: Capacitor C pre-charging during first 2 cycles. Legend: Blue – power line voltage, Red - voltage on Capacitor C in respect to common Ground, Yellow – driver to Sw1, Green – Capacitor current. (Not to scale)

During Cycle 1, Sw1 is in ON state (conducting) from time t1 to T shown in Figure 2. The voltage across the capacitor increases to voltage proportional to normalized value 1/N. During this period, the charging current rising would follow the LC resonant behavior as shown in Figure 3 (green line). The current is rising until the capacitor voltage reaches input voltage, excluding voltage dropouts, then the current continues its resonant behavior as long as Sw1 is ON. No further oscillation occurs because input voltage drops below voltage on capacitor, and then Sw1 is OFF (not conducting). Capacitor remains pre-charged to the voltage proportional to 1/N. In Cycle 2, Capacitor C is pre-charged by another voltage increment 1/N in the process similar to Cycle 1. Capacitor C is charged N cycles to the voltage value proportional to the input line voltage.

## Composing Timing for Digital Inrush Control

A simplified timing diagram for inrush control is shown in Figure 2 in which the voltage increment for each cycle is defined by the number of cycles N. The capacitor charging current is proportional to voltage increment, 1/N. Hence, the number of cycles N is the variable to control peak inrush current. Another variable to control inrush current is LC time constant. Capacitor C value depends on desired ripple value. After selecting the capacitor C value, the designer can decrease peak inrush current by increasing inductance L. If there are physical limits to L value, the number of cycles N should be used to set the required peak current. Turn ON time for Switch Sw1 should be defined for each active cycle. Assuming that delay from zero crossing (point 0 in Figure 2) to the beginning of turning Sw1 ON, t4, is $\boldsymbol{T_{off}}$ , an active time to keep Sw1 ON is $\boldsymbol{T_{on}}$, and cycle duration is $\boldsymbol{T}$**, c**ycles are defined as
$\boldsymbol{T_{on}}$ for each occurrence $\boldsymbol{i}$ is defined as geometrical transform

$$\boldsymbol{T_{on(i)}} = \frac{\boldsymbol{T}}{\boldsymbol{\pi/2}}\,\textbf{asin}\,(\boldsymbol{i/N}), \quad where\ i = 1 \ldots N \quad (1)$$

The period $\boldsymbol{T}$ is measured by MCU at initialization. Values $\boldsymbol{T_{on}}$ are determined by (1) and stored in memory. Values for $\boldsymbol{T_{off}}$ are derived by firmware according to following expression

$$\boldsymbol{T_{off(i)}} = \boldsymbol{T} - \boldsymbol{T_{on(i)}} \quad (2)$$

Figure 4 illustrates how $\boldsymbol{T_{on(i)}}$ values are defined for 16 cycles used in this reference design for 120V@60Hz. Blue line (rectified power line voltage) is shown for reference. Magenta represents actual $\boldsymbol{T_{on}}$ time value in µs for each cycle, and yellow is $\boldsymbol{T_{on}}$ pulse positioned relatively to rectified power line voltage. Figure 4 conceptually illustrates algorithm behavior as it is executed in MCU Z8F3281. Timing counter (red line) corresponds to time at any given moment of discrete time base provided by internal clock. The counter first counts till $\boldsymbol{T_{off}}$ value represented by green line. When counter reaches $\boldsymbol{T_{off}}$ value it initiates $\boldsymbol{T_{on}}$ pulse (yellow line) which continues according to counter reaches $\boldsymbol{T_{on}}$ value (magenta line).

An illustration of timing position and amplitude of capacitor C current (green) with respect to $\boldsymbol{T_{on}}$ pulses is depicted on Figure 5. It is noted that only single current pulse is produced by Inrush Controller during a cycle because after capacitor charge is completed input voltage drops below capacitor voltage and input power line is isolated from the rest of the circuitry by diode bridge. Inductor discharges into capacitor, then switch Sw1 is off (not conducting) at the end of the cycle.

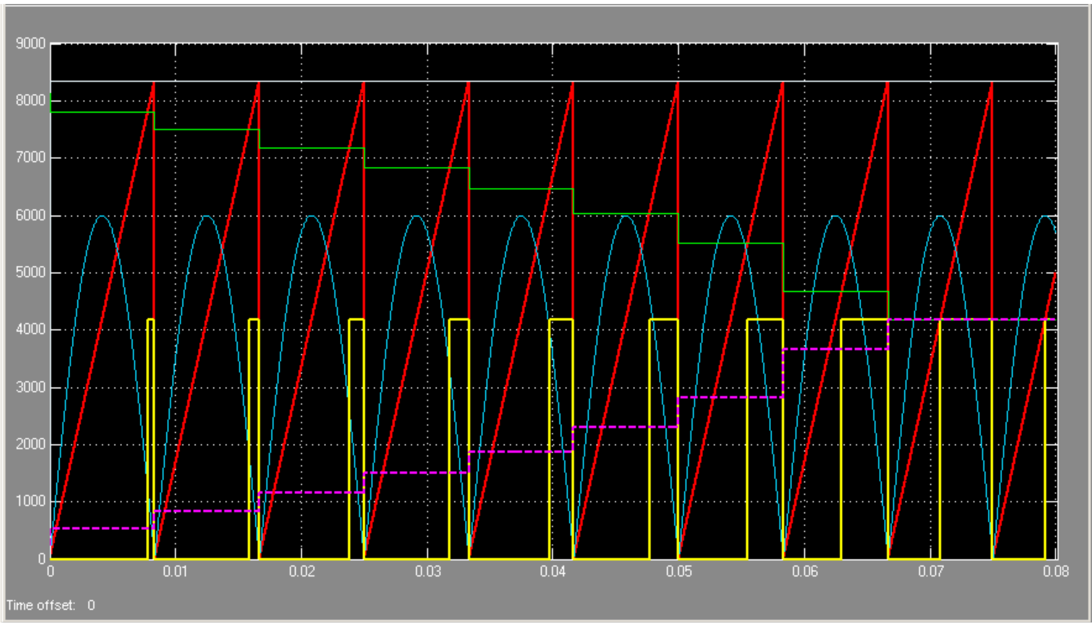


Figure 4: $T_{on}$ timing generation. Legend: Blue – rectified power line voltage, Red – full cycle period timing counter, Yellow – driver to Sw1, Green – time OFF to Sw1, Magenta – Time ON to Sw1, White – period T.

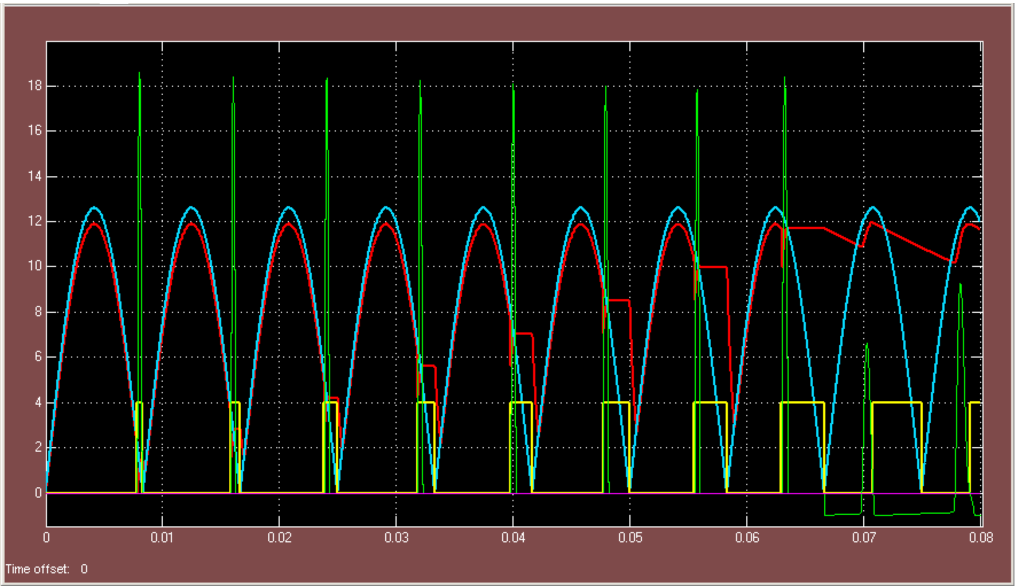


Figure 5: Capacitor C pre-charging. Legend: Blue – rectified power line voltage, Red – voltage Capacitor C in respect to common Ground, Yellow – driver to Sw1, Green – Capacitor current.

## Discussion of Hardware Implementation

This Digital Inrush Controller consists of MCU module and power components board shown in Figure 6(a) and 6 (b). The MCU Module is implemented as add-on device. The module comprises connector J4 for MCU programming. MCU should be programmed before powering the entire Inrush Controller. If Inrush Controller is powered before programming MCU the result is unpredictable. The Digital Control Module is powered by Auxiliary power supply +3.3V for MCU and 12V for gate driver applied to the connector J4 on the Power Board.

The Power Board is a two-layer surface-mount device that provides easy access to test points. Diode Bridge BR1 (see Appendix 1 for schematic), MOSFETs Q1, Q2, and Q3 are mounted on small heat sinks. Power dissipated on these heat sinks is less than 5 W at 375 W output power. This Board may be powered from 50 or 60 Hz AC source. Figure 6 displays a view of the Board’s power components.

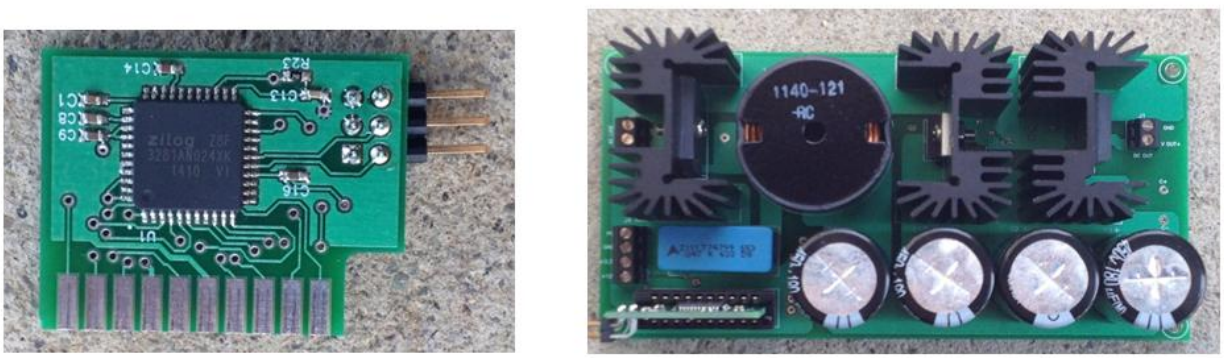


(a) (b)

Figure 6: (a) MCU module and (b) Digital Inrush Controller with MCU module

## Setup and Test results

Performance of the Reference Design had been programmed and verified on a test bench as shown on Figure 7. AC line input was fed through 0.5 kW isolation transformers. The load is designed to consume 2.5A at normal operation. To test overload conditions additional load was used to provide 3.5A. Instantaneous connection of additional load was enough to trigger overload protection. Continuous overload results in multiple attempts to restart device with immediate interruption.

Auxiliary Power Supply should be turned ON after AC power is ON. After power-on reset and initialization, MCU analyses power line, sets appropriate timing, and begin pre-charging of bulk capacitor. Actual waveforms taken from a scope at normal operation are depicted on figure 8.

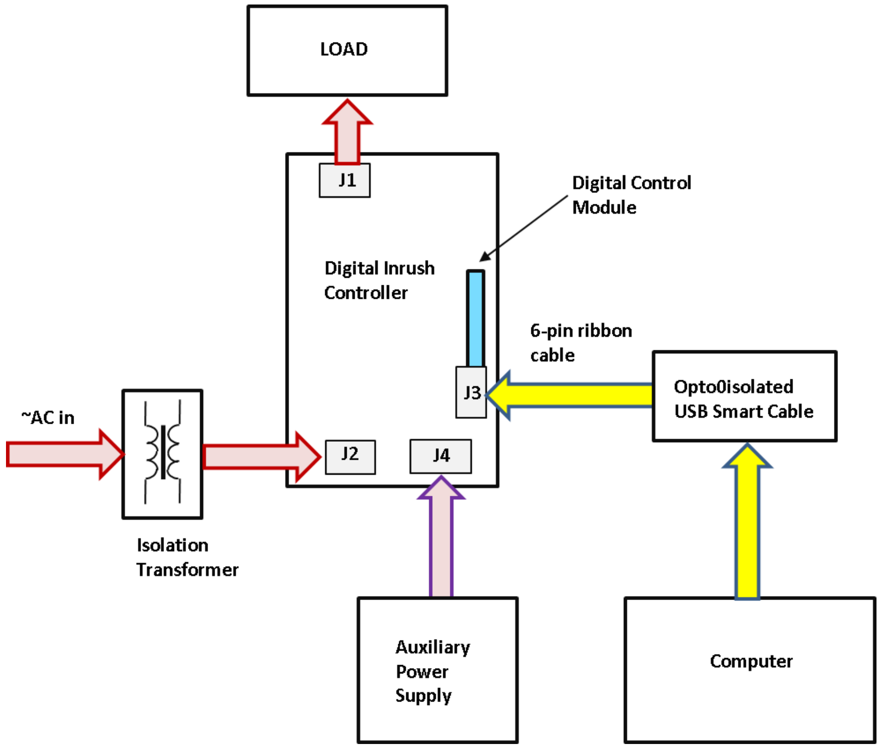


Figure 7: Digital Inrush Controller Setup

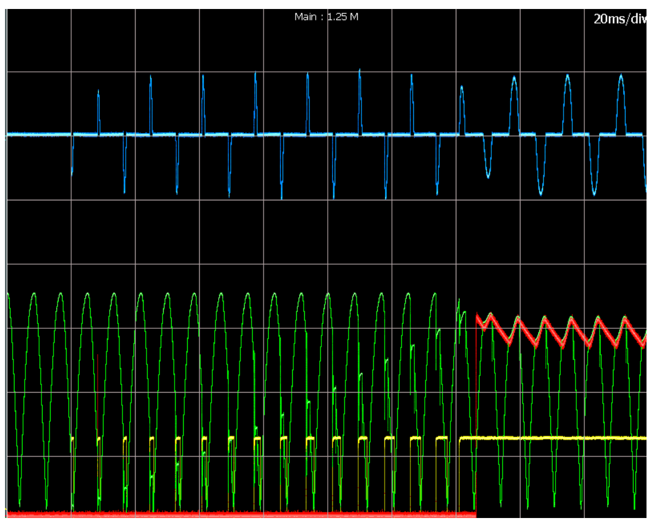


Figure 8: Scope snapshot of the Digital Inrush Current Control. Legend: Blue – power line current (10A/div), Red – Load voltage (50V/div), Green – rectified input voltage (50V/div), Yellow –Sw1 commutation signal.

Inrush current (top blue line) is limited to 10A. Yellow line shows signal at Sw1 gate. After inrush procedure is finished, gate is set to high level to keep Sw1 conducting. On cycle later load is connected and load voltage rises from zero to the level on pre-charged capacitor.

Slight drop in the rectified voltage after load is connected happens due to limited power capability of the isolation transformer. To illustrate performance of increasing number of inrush control cycles at the same power conditions, measurements were done with controller reprogrammed to 16 cycles instead of original 8. The inrush current dropped 2 times as it is shown on Figure 9.

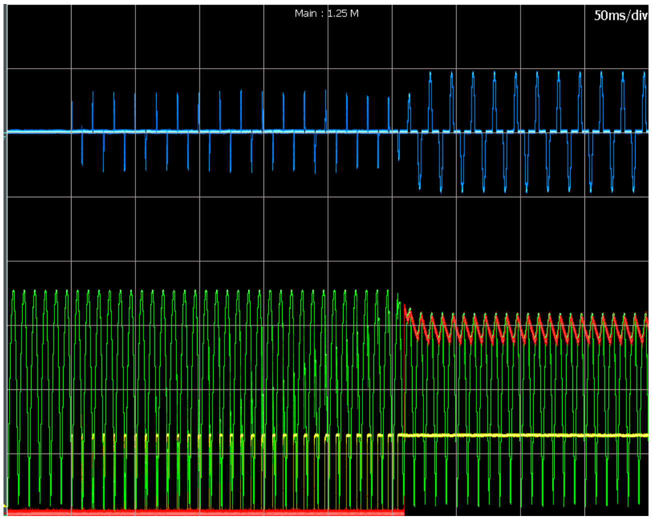


Figure 9: Scope snapshot of inrush pulses with N increased to 16. Legend: Blue – power line current (10A/div), Red – Load voltage (50V/div), Green – rectified input voltage (50V/div), Yellow – driver to Sw1.

## Performance at overload conditions

Normal operation starts with pre-charging of bulk capacitor. Startup is shown on Figure 10 with a horizontal scale of 1s. Yellow line indicating gate driver state is wide because of the low graphic resolution for 12 cycles of pre-charge. After inrush control sequence is over, load is connected – red line goes up – and then Power Good status (blue line) goes up as well. Continuous overload is applied at 2.3 seconds. Load is disconnected and Power Good status goes low. Attempt to restart device initiated in 1.5 second interval. Inrush sequence is performed again, then load is connected, but overload is sensed right away, load is disconnected, and Power Good status continues to stay low. Another attempt to restart is repeated in 1.5 seconds and load stay connected for about 1 second while there is no overload condition.

## Results

Upon testing, this reference design achieved its goal of digital inrush control by harnessing the capabilities of embedded control by implementing unique algorithms. Testing of this design showed the following results:

- Inrush current is limited to predefined value
- High efficiency in 99.5% range
- Wide input voltage range: 80V to 240V

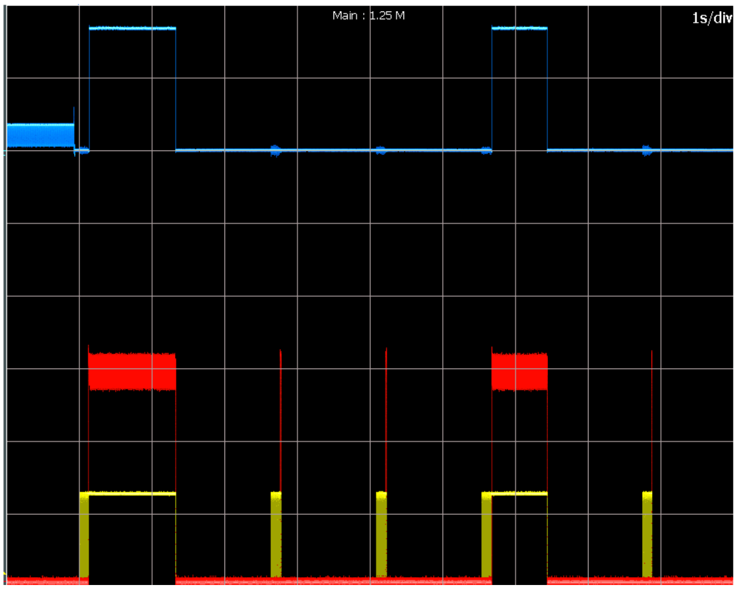


Figure 10: Scope snapshot to illustrate Overload and restart. Legend: Blue –Power Good status, Red – Load voltage (50V/div), Yellow – driver to Sw1.

- Wide input frequency range: 50/60/400Hz
- Option to turn Load ON/OFF
- Programmable Overload protection: number of overload instances, period between overload event, continuous overload or instant
- Power Good status, which is not present in overload conditions
- Not sensitivity to Power interruptions, brownout
- Not sensitivity to temperature variations
- High endurance

## Conclusion

Digital Inrush Controller based on Zilog's F3281 Series of MCUs, offers flexibility in implementing a unique control algorithm that aids in efficient power system. It achieves a high level of efficiency, increased stability, and reliable performance across a wide load range. Because of an innovative current measurement algorithm, this Controller allows common input and load grounds. Users can optimize the system for a wide range of input voltages and frequencies. This design provides instant over-current protection, followed by an intervention by the MCU for corrective actions. This Controller can be used as a part of AC-DC rectifier or can be expanded to a high level application like PFC converter. Digital control can be used to build a user interface that would allow users to change device parameters, gather statistics, add a communication interface, remotely monitor performance, or change parameters.

# Appendix A: Schematic Diagrams

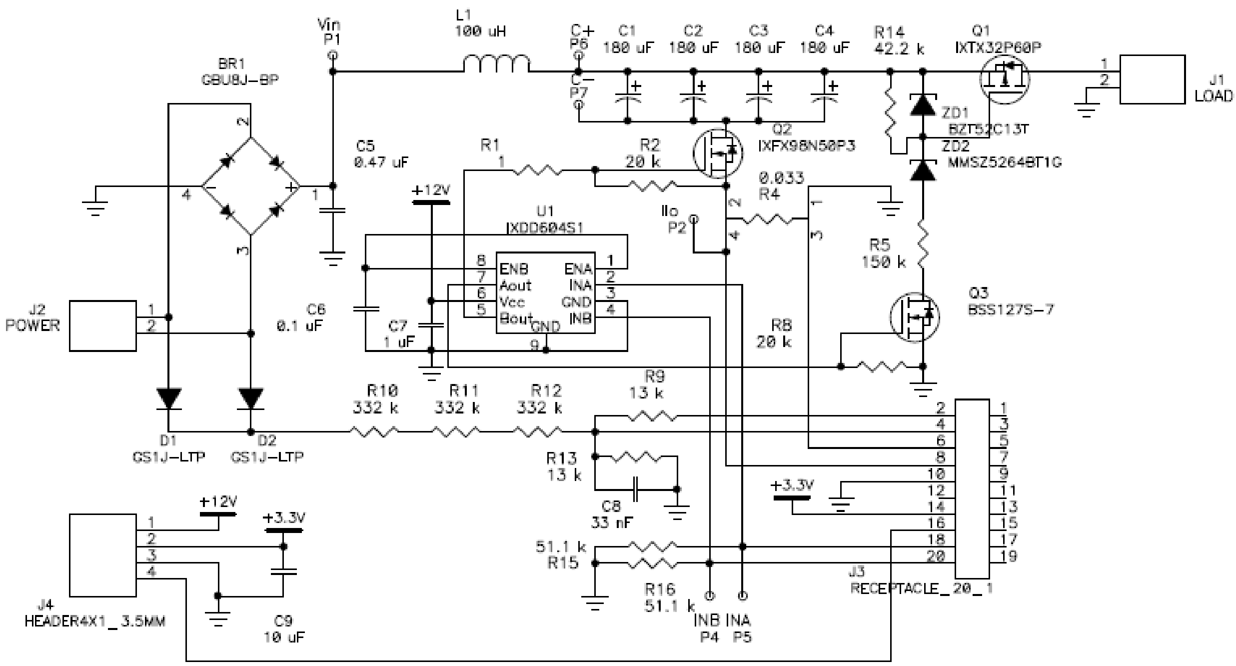


Figure 11: Schematic Diagram of Digital Inrush Controller main board

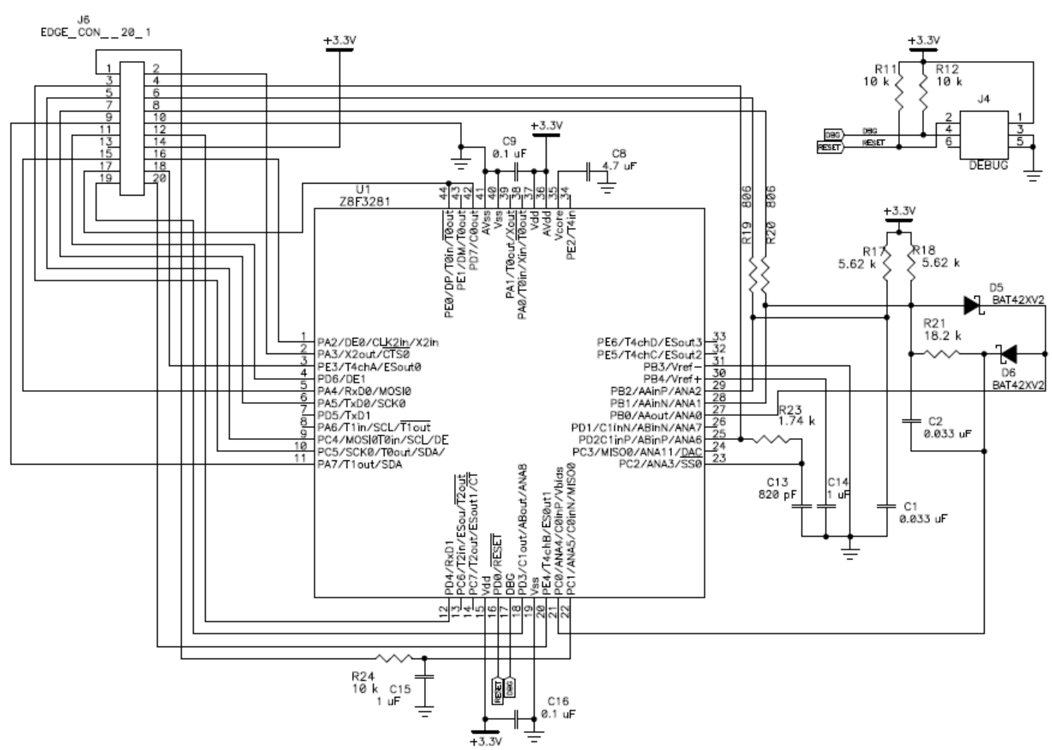


Figure 12: Schematic Diagram of Digital Control module

# Appendix B: Bill of Materials (BOMs)

Table 1 and table 2 list the components used to build this reference design board.

**Table 1: Components of Digital MCU Module**

| Count | Reference Designator | Value | Description | Manufacturer |
|---|---|---|---|---|
| | | | | |
| 2 | C1, C2 | 0.033 µF | C0603C333K4RACTU | Kemet |
| 2 | C9, C16 | 0.1 µF | CL10B105KA8NNNC | Samsung |
| 2 | C14, C15 | 1 µF | CL10B106KA8NNNC | Samsung |
| 1 | C8 | 4.7 µF | CL10A475KA8NQNC | Samsung |
| 1 | C13 | 820 pF | TMK107B7821KA-T | Taiyo Yuden |
| 2 | D5, D6 | BAT42XV2 | BAT42XV2 | Diodes Inc. |
| 1 | J6 | | Board Layout | |
| 1 | J4 | | Header 67996-406HLF | FCI |
| 1 | R23 | 1.74 k | RMCF0603FT1K74 | Stackpole Electronics Inc |
| 2 | R17, R18 | 5.62 k | RMCF0603FT5K62 | Stackpole Electronics Inc |
| 3 | R11, R12, R24 | 10 k | RMCF0603FT10K0 | Stackpole Electronics Inc |
| 1 | R21 | 18.2 k | RMCF0603FT18K2 | Stackpole Electronics Inc |
| 2 | R19, R20 | 806 | RMCF0603FT806R | Stackpole Electronics Inc |
| 1 | U1 | Z8F3281 | Z8F3281AN024XK | Zilog |

**Table 2: Main Board Components**

| Count | Reference Designator | Value | Description | Manufacturer |
|---|---|---|---|---|
| | | | | |
| 1 | BR1 | GBU8J-BP | GBU8J-BP | Micro Commercial Co with HS |
| 3 | BR1, Q1, Q2 | 6398BG | Heat Sink | Aavid Thermalloy |
| 4 | C1, C2, C3, C4 | 180 µF | ESMQ451VSN181MP40S | United Chemi-Con |
| 1 | C5 | 0.47 µF | B32653A6474K | EPCOS Inc |
| 1 | C6 | 0.1 µF | C0603C104K3RACTU | Kemet |
| 1 | C7 | 1 µF | TMK107B7105KA-T | Taiyo Yuden |
| 1 | C8 | 33 nF | C0603C333K3RACTU | Kemet |
| 1 | C9 | 10 µF | CL10A106MA8NRNC | Samsung |
| 2 | D1, D2 | GS1J-LTP | GS1J-LTP | Micro Commercial Co |
| 2 | J1, J2 | | Terminal Block 39357-0002 | Molex |
| 1 | J3 | | 5-5530843-0 | TE Connectivity |
| 1 | J4 | | Terminal Block 39357-0004 | Molex |
| 1 | L1 | 100 µH | 1140-101K-RC | Bourns Inc. |
| 7 | P1 –P7 | | 1001-0-15-01-30-02-04-0 | Mill-Max |
| 1 | Q1 | IXTX32P60P | IXTX32P60P | IXYS Corp. with HS |
| 1 | Q2 | IXFX98N50P3 | IXFX98N50P3 | IXYS Corp. with HS |
| 1 | Q3 | BSS127S-7 | BSS127S-7 | Diodes Incorporated |
| 1 | R1 | 1 | CRCW06031R00FSTA | Vishay |
| 3 | R10, R11, R12 | 332 k | RMCF1206FT332K | Stackpole Electronics Inc |
| 1 | R14 | 42.2 k | RMCF0603FT42K2 | Stackpole Electronics Inc |
| 2 | R15, R16 | 51.1 k | RMCF0603FT51K1 | Stackpole Electronics Inc |
| 2 | R2, R8 | 20 k | RMCF0603FT20K0 | Stackpole Electronics Inc |
| 1 | R4 | 0.033 | LVK24R033FER | Ohmite |
| 1 | R5 | 150 k | ERJ-14NF1503U | Panasonic Electronic Comp. |
| 2 | R9, R13 | 13 k | RMCF0603FT13K0 | Stackpole Electronics Inc |
| 1 | U1 | | IXDD604S1 | IXYS Corp. |
| 1 | ZD1 | BZT52C13T | BZT52C13T-7 | Diodes Inc. |
| 1 | ZD2 | MMSZ5264BT1G | MMSZ5264BT1G | ON Semiconductor |